On the Thermodynamics of Particle-Stabilized Emulsions: Curvature Effects and Catastrophic Phase Inversion

P. A. Kralchevsky,*,† I. B. Ivanov,† K. P. Ananthapadmanabhan,‡ and A. Lips‡

Laboratory of Chemical Physics & Engineering, Faculty of Chemistry, University of Sofia, 1164 Sofia, Bulgaria, and Unilever Research US, 45 River Road, Edgewater, New Jersey 07020

Received September 3, 2004. In Final Form: October 19, 2004

The flexural properties of a particle adsorption monolayer are investigated theoretically. If the particles are not densely packed, the interfacial bending moment and the spontaneous curvature (due to the particles) are equal to zero. The situation changes if the particles are closely packed. Then the particle adsorption monolayer possesses a significant bending moment, and the interfacial energies of bending and dilatation become comparable. In this case, the bending energy can either stabilize or destabilize the Pickering emulsion, depending on whether the particle contact angle is smaller or greater than 90°. Theoretical expressions are derived for the bending moment, for the curvature elastic modulus, and for the work of interfacial deformation and emulsification. The latter is dominated by the work for creation of a new oil−water interface and by the work for particle adsorption. The curvature effects give a contribution of second order, which is significant only for emulsification at 50:50 water/oil volume fractions. A thermodynamic criterion for the type of the formed emulsion is proposed. It predicts the existence of a catastrophic phase inversion in particle-stabilized emulsions, in agreement with the experimental observations. The derived theoretical expressions could find application for interpretation of experimental data on production and stability of Pickering emulsions.

1. Introduction

Colloidal particles, adsorbed at the oil−water interface serve as stabilizers of emulsions, the so-called Pickering emulsions.[1] The dense particle adsorption monolayers provide steric hindrance to drop−drop coalescence.[2] Comprehensive recent reviews on formation, stability, and applications of Pickering emulsions were published by Binks[3] and Aveyard et al.[4]

Experimentally, silica,[5−8] clay,[9−11] and latex[12−15] particles have been used as emulsion stabilizers. Sometimes the system contains both particles and amphiphilic molecules (surfactants, block copolymers).[7,10,16] At not too high concentrations, the amphiphile could modify the contact angle of the adsorbed particles and thus influence the type and stability of the formed emulsion.[7] (At higher concentrations, the surfactant itself, rather than the particles, could stabilize the emulsion.) The effects of particle size[12] and wettability[5−7] on the properties of the formed emulsions have been examined experimentally. A catastrophic phase inversion of water-in-oil emulsions was observed upon variation of the volume fraction of water.[17] Model experiments were carried out to investigate the particle interactions and self-assembly at the fluid interface[18−25] and to reveal the mechanism of flocculation and coalescence in the Pickering emulsions.[26−28]

Theoretically, the properties of liquid films stabilized by solid particles were investigated,[29,30] and the lateral capillary forces between particles captured in such films were examined.[31] A theoretical treatment was developed to calculate the solid−water−oil contact angles for oils of different polarity.[32] As the effect of line tension could affect

* Corresponding author: Phone: (+359) 2-962 5310. Fax: (+359) 2-962 5438. E-mail: pk@lcpe.uni-sofia.bg.

† University of Sofia.

‡ Unilever Research US.

(1) Pickering, S. U. *J. Chem. Soc*. **1907**, *91*, 2001.
(2) Tambe, D. E.; Sharma, M. M. *Adv. Colloid Interface Sci.* **1994**, *52*, 1.
(3) Binks, B. P. *Curr. Opin. Colloid Interface Sci.* **2002**, *7*, 21.
(4) Aveyard, R.; Binks, B. P.; Clint, J. H. *Adv. Colloid Interface Sci.* **2003**, *100−102*, 503.
(5) Binks, B. P.; Lumsdon, S. O. *Langmuir* **2000**, *16*, 3748.
(6) Binks, B. P.; Lumsdon, S. O. *Langmuir* **2000**, *16*, 8622.
(7) Kruglyakov, P. M.; Nushtayeva, A. V.; Vilkova, N. G. *J. Colloid Interface Sci.* **2004**, *276*, 465.
(8) Vignati, E.; Piazza, R.; Lockhart, T. P. *Langmuir* **2003**, *19*, 6650.
(9) Abend, S.; Bonnke, N.; Gutschner, U.; Lagaly, G. *Colloid. Polym. Sci.* **1998**, *276*, 730.
(10) Lagaly, G.; Reese, M.; Abend, S. *Appl. Clay Sci*. **1999**, *14*, 83.
(11) Thieme, J.; Abend, S.; Lagaly, G. *Colloid. Polym. Sci.* **1999**, *277*, 257.
(12) Binks, B. P.; Lumsdon, S. O. *Langmuir* **2001**, *17*, 4540.
(13) Giermanska-Kahn, J.; Schmitt, V.; Binks, B. P.; Leal-Calderon, F.; *Langmuir* **2002**, *18*, 2515.
(14) Binks B. P.; Kirkland, M. *Phys. Chem. Chem. Phys*. **2002**, *4*, 3727.
(15) Tarimala, S.; Dai, L. L. *Langmuir* **2004**, *20*, 3492.
(16) Gosa, K. L.; Uricanu V. *Colloids Surf., A* **2002**, *197*, 257.
(17) Binks, B. P.; Lumsdon, S. O. *Langmuir* **2000**, *16*, 2539.
(18) Velev, O. D.; Furusawa, K.; Nagayama, K. *Langmuir* **1996**, *12*, 2374.
(19) Velikov K. P.; Durst, F.; Velev, O. D. *Langmuir* **1998**, *14*, 1148.
(20) Dinsmore, A. D.; Hsu, M. F.; Nikolaides, M. G.; Marquez, M.; Bausch, A. R.; Weitz, D. A. *Science* **2002**, *298*, 1006.
(21) Nikolaides, M. G.; Bausch, A. R.; Hsu, M. F.; Dinsmore, A. D.; Brenner, M. P.; Gay, C.; Weitz, D. A. *Nature* **2002**, *420*, 299.
(22) Aveyard, R.; Binks, B. P.; Clint, J. H.; Fletcher, P. D. I.; Horozov, T. S.; Neumann, B.; Paunov, V. N.; Annesley, J.; Botchway, S. W.; Nees, D.; Parker, A. W.; Ward, A. D.; Burgess, A. *Phys. Rev. Lett*. **2002**, 88, 246102−1−4.
(23) Horozov, T. S.; Aveyard, R.; Clint, J. H.; Binks, B. P. *Langmuir* **2003**, *19*, 2822.
(24) Danov, K. D.; Kralchevsky, P. A.; Boneva, M. P. *Langmuir* **2004**, *20*, 6139.
(25) Tarimala, S.; Ranabothu, S. R.; Vernetti, J. P.; Dai, L. L. *Langmuir* **2004**, *20*, 5171.
(26) Ashby, N. P.; Binks, B. P.; Paunov, V. N. *Chem. Commun.* **2004**, 436−437.
(27) Stancik E. J.; Kouhkan, M.; Fuller, G. G. *Langmuir* **2004**, *20*, 90.
(28) Stancik E. J.; Fuller, G. G. *Langmuir* **2004**, *20*, 4805.
(29) Denkov, N. D.; Ivanov, I. B.; Kralchevsky, P. A.; Wasan, D. T. *J. Colloid Interface Sci*. **1992**, *150*, 589.
(30) Nushtayeva, A. V.; Kruglyakov, P. M. *Mendeleev Commun.* **2001** (6), 235−237; *Colloid J*. **2003**, *65*, 341.
(31) Danov, K. D.; Pouligny, B.; Kralchevsky, P. A. *Langmuir* **2001**, *16*, 6599.
(32) Binks, B. P.; Clint, J. H. *Langmuir* **2002**, *18*, 1270.

10.1021/la047793d CCC: $30.25
Published on Web 12/07/2004

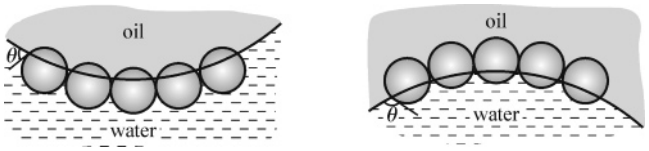

Figure 1. Contact angle and emulsion type: The experiment shows that hydrophilic particles ($\theta < 90°$) stabilize oil-in-water emulsions, while hydrophilic particles ($\theta > 90°$) stabilize water-in-oil emulsions. A possible reason for this effect could be the curvature energy of the particle adsorption layer.[3,4,35]

the particle contact angle for nanoparticles,[33,34] its influence on the free energy of drop formation in the Pickering emulsions has been also analyzed.[4,35] The equilibrium contact angle, θ, determines the position of stable attachment of a particle to the oil−water interface, which corresponds to a minimum of the system's free energy.[29] (Note, however, that if the oil drop is replaced by a gas bubble, the equilibrium contact angle could correspond to a maximum of the free energy, i.e., to unstable equilibrium.[36,37] The latter fact could have implications for Pickering foams.) Theoretical comparison was made between spheres of uniform wettability and amphiphilic "Janus" particles, with respect to their adsorption/desorption properties at an oil−water interface.[38]

Recently, attention was paid also to the curvature energy of particle adsorption monolayers.[3,4,35] The experiment shows that typically, oil-in-water (o/w) Pickering emulsions are formed for $\theta < 90°$, while water-in-oil (w/o) emulsions are obtained for $\theta > 90°$ (here, θ is measured across the water phase). This fact correlates with the interfacial curvature effects: By analogy with surfactant molecules, the monolayers will curve such that the larger area of the particle surface remains on the external side, giving rise to o/w emulsions when $\theta < 90°$ and w/o emulsions when $\theta > 90°$; see Figure 1 and refs 3 and 4. However, the question whether the curvature (bending) energy really determines the emulsion type, or the two factors only correlate because both of them are governed by a third factor, needs additional investigation.

Here, our goal is to study theoretically, in more detail, the effect of the interfacial bending energy and particle adsorption energy on emulsification and emulsion stability. We present a quasi-equilibrium *thermodynamic* model and investigate its predictions. The latter could agree or disagree with the experimental observations depending on whether additional *kinetic* effects are absent or present. We believe that such thermodynamic study is a necessary first step toward development of a quantitative theory, which takes into account both the thermodynamic and kinetics aspects of the investigated processes.

In sections 2 and 3, we derive explicit expressions for the interfacial bending moment, B_0, and the bending elasticity, k_s. Next, we compare the works of bending and dilatation, ΔW_b and ΔW_{dil}, carried out during the deformation upon collision of two emulsion drops. In section 4, we consider the work of emulsification, i.e., breaking of the disperse phase to an increasing number of drops (of diminishing size), which is accompanied by particle adsorption at the newly created oil−water interface. We calculate separately the works for production of the direct and reverse emulsions, W_1 and W_2, with account for the curvature effects. In section 5, we establish that the sign of the difference, $\Delta W = W_1 - W_2$, could serve as a thermodynamic criterion about the type of the formed emulsion (o/w or w/o).

In this paper, our attention is focused on the influence of three main factors: (i) the contact angle, (ii) the bending energy, and (iii) the volume fractions of oil and water in the emulsion. For simplicity, we assume that the solid particles are spherical and monodisperse and their surfaces have uniform wettability. Moreover, some effects, as the adsorption entropy and the line tension, which could be essential for very small particles,[4] are neglected in our thermodynamic analysis. The consideration of a possible effect of contact-angle hysteresis[39−42] is postponed for subsequent studies.

Let us mention in advance that the bending energy really turns out to be important for the emulsion *stability*, supposedly the particles in the adsorption monolayers are closely packed (section 3). What concerns the *emulsification work*, the curvature effects give only a second-order contribution, the major factor being the volume fraction of water and oil (section 4).

As mentioned above, the occurrence and result of emulsification are influenced also by kinetic factors, such as the characteristic times of particle adsorption and of drop−drop collision (see section 5.3). The effects of these kinetic factors can be identified as deviations from the predictions of the thermodynamic model and could be further interpreted in terms of emulsification hydrodynamics[43−46] and kinetic barriers to particle adsorption at the oil−water interface.[47,48]

2. Bending of a Non-Closely-Packed Particle Monolayer

2.1. Basic Equations. Let us consider a portion of a spherical oil−water interface with adsorbed spherical particles; see Figure 2. This could be a portion of the surface of a drop in a Pickering emulsion. The respective surface free energy can be written in the form

$$W = \sigma_{12}A_{12} + \sigma_{1p}A_{1p} + \sigma_{2p}A_2 \qquad (2.1)$$

Here, A_{12} is the boundary between the inner phase 1 and the outer phase 2, which are either water or oil, depending on the type of the emulsion, o/w or w/o; A_{1p} and A_{2p} are the total areas particle/phase 1 and particle/phase 2; and σ_{12}, σ_{1p}, and σ_{2p} are the respective interfacial tensions. We assume that there is no contact-angle hysteresis and, consequently, the Young equation is satisfied

$$\sigma_{1p} - \sigma_{2p} = \sigma_{12}\cos\theta \qquad (2.2)$$

(33) Widom, B. *J. Phys. Chem.* **1995**, *99*, 2803.
(34) Gaydos, J.; Neumann, A. W. In *Applied Surface Thermodynamics*; Neumann, A. W., Spelt, J. K., Eds.; Marcel Dekker: New York, 1996; Chapter 4, p 169.
(35) Aveyard, R.; Clint, J. H.; Horozov, T. S. *Phys. Chem. Chem. Phys.* **2003**, *5*, 2398.
(36) Eriksson, J. C.; Ljunggren, S. *Langmuir* **1995**, *11*, 2325.
(37) Eriksson, J. C.; Ljunggren, S. *Colloids Surf., A* **1999**, *159*, 159.
(38) Binks, B. P.; Fletcher, P. D. I. *Langmuir* **2001**, *17*, 4708.
(39) Johnson, R. E., Jr.; Dettre, R. H. *J. Phys. Chem.* **1964**, *68*, 1744.
(40) Eick, J. D.; Good, R. J.; Neumann, A. W. *J. Colloid Interface Sci.* **1975**, *53*, 235.
(41) Finn, R.; Shinbrot, M. *J. Math. Anal. Appl.* **1987**, *123*, 1.
(42) Kralchevsky, P. A.; Nagayama, K. *Particles at Fluid Interfaces and Membranes*; Elsevier: Amsterdam, The Netherlands, 2001.
(43) Walstra, P. In *Encyclopedia of Emulsion Technology*; Becher, P., Ed.; Marcel Dekker: New York, 1983; Chapter 2.
(44) Walstra, P.; Geurts, T. J.; Noomen, A.; Jellema, A.; van Boekel, M. A. J. S. *Dairy Technology*; Marcel Decker: New York, 1999.
(45) Narsimhan, G. *J. Colloid Interface Sci.* 2004, *272*, 197.
(46) Tcholakova, S.; Denkov, N. D.; Danner, T. *Langmuir* **2004**, *20*, 7444.
(47) Hadjiiski, A.; Tcholakova, S.; Denkov, N. D.; Durbut, P.; Broze, G.; Mehreteab, A. *Langmuir* **2001**, *17*, 7011.
(48) Hadjiiski, A.; Denkov, N. D.; Tcholakova, S.; Ivanov, I. B. In *Adsorption and Aggregation of Surfactants in Solution*; Mittal K. L., Shah D. O., Eds.; Marcel Dekker: New York, 2002; p 465.

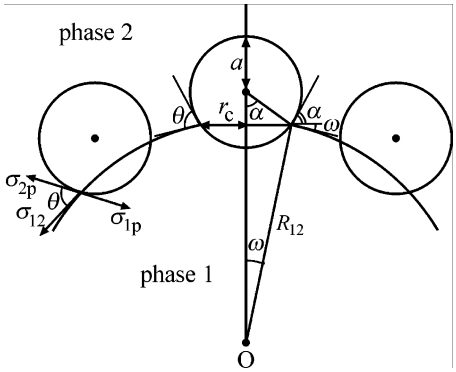

Figure 2. Sketch of spherical particles at the surface of an emulsion drop from phase 1 surrounded by phase 2. The notations are explained in the text.

For a spherical interfacial segment of area A, the areas taking part in eq 2.1 are

$$A_{12} = A - 2\pi R_{12}{}^2(1 - \cos\omega)N_p \tag{2.3a}$$

$$A_{1p} = 2\pi a^2(1 - \cos\alpha)N_p \tag{2.3b}$$

$$A_{2p} = 2\pi a^2(1 + \cos\alpha)N_p \tag{2.3c}$$

where N_p is the number of adsorbed monodisperse particles, a is their radius, and $\sin\alpha = r_c/a$; the angles α and ω are shown in Figure 2; r_c is the radius of the contact line on the particle surface. The substitution of eqs 2.2–2.3 into eq 2.1 yields

$$W = \sigma_{12}A_{12} - 2\pi a^2 N_p \sigma_{12}\cos\theta\cos\alpha + 2\pi a^2 N_p(\sigma_{1p} + \sigma_{2p}) \tag{2.4}$$

The last term in eq 2.4 is constant and does not contribute to the bending energy. As illustrated in Figure 2, $\theta = \alpha + \omega$ and $r_c = a\sin\alpha = R_{12}\sin\omega$. Thus, we have two equations to determine the angles α and ω

$$\alpha = \theta - \omega, \qquad \sin\omega = \epsilon\sin(\theta - \omega) \tag{2.5}$$

$$\epsilon \equiv a/R_{12} \ll 1 \tag{2.6}$$

From eq 2.5 we get

$$\tan\omega = \frac{\epsilon\sin\theta}{1 + \epsilon\cos\theta} = \epsilon\sin\theta - \epsilon^2\sin\theta\cos\theta + ... \tag{2.7}$$

where we have used a series expansion and the fact that $\epsilon \ll 1$. Having in mind that $\sin\omega = \epsilon\sin\alpha$, and using eq 2.7, we bring eq 2.3a in the form

$$A_{12} = A - \pi a^2\left(\sin^2\alpha + \frac{1}{4}\epsilon^2\sin^4\alpha\right)N_p \tag{2.8}$$

The thermodynamics yields the following expression for the work of interfacial deformation;[49–51] see also Chapter 3 in ref 42

$$\mathrm{d}W/A = \sigma\,\mathrm{d}\tilde{\alpha} + B\,\mathrm{d}H \tag{2.9}$$

where $\mathrm{d}\tilde{\alpha} = \mathrm{d}A/A$ is the interfacial dilatation, B is the interfacial bending moment, and $H = -1/R_{12}$ is the mean curvature of the oil–water interface. By definition A is the area of a given selected parcel on the sphere of radius R_{12}; this sphere passes over the oil–water interface between the particles (Figure 2).

2.2. The Interfacial Bending Moment. From eq 2.9 it follows

$$B = \frac{1}{A}\left(\frac{\partial W}{\partial H}\right)_{\tilde{\alpha}} = \left(\frac{\partial(W/A)}{\partial H}\right)_{\tilde{\alpha}} \tag{2.10}$$

The variation of H at fixed $\tilde{\alpha}$ is equivalent to a variation of the radius R_{12} (Figure 2) at fixed area, A, of the selected parcel on the oil–water interface, which contains a given number, N_p, of adsorbed particles. In such a case, the particle adsorption, $\Gamma = N_p/A$, will be also constant. Then, from eqs 2.4 and 2.8 we get

$$\frac{W}{A} = \sigma_{12} - \sigma_{12}\Gamma\pi a^2\left(\sin^2\alpha + \frac{1}{4}\epsilon^2\sin^4\alpha + 2\cos\theta\cos\alpha\right) + \text{constant} \tag{2.11}$$

The contact angle θ is presumed to be constant, and then the dependence of W/A on R_{12} comes through the angle α. Since $\theta - \alpha = \omega \ll 1$, we obtain

$$\cos\alpha = \cos\theta - \left.\frac{\partial\cos\alpha}{\partial\alpha}\right|_{\alpha=\theta}\omega + \frac{1}{2}\left.\frac{\partial^2\cos\alpha}{\partial\alpha^2}\right|_{\alpha=\theta}\omega^2 + ... \tag{2.12}$$

In view of eq 2.7, we can represent eq 2.12 in the form

$$\cos\alpha = \cos\theta + \epsilon\sin^2\theta - \frac{3}{2}\epsilon^2\sin^2\theta\cos\theta + O(\epsilon^3) \tag{2.13}$$

Substituting eq 2.13 into eq 2.11, after some transformations, we obtain

$$\frac{W}{A} = \sigma_{12} - \sigma_{12}\varphi_a\left(1 + \cos^2\theta - \frac{3}{4}\epsilon^2\sin^4\theta\right) + O(\epsilon^3) + \text{constant} \tag{2.14}$$

where $\varphi_a = \Gamma\pi a^2$ characterizes the area fraction occupied by the adsorbed particles. Note that in eq 2.14, a linear term, proportional to ϵ, is missing. Having in mind that $\epsilon = -aH$, we differentiate eq 2.14, in accordance with eq 2.10, and derive the following expression for the bending moment

$$B = \frac{3}{2}\sigma_{12}\varphi_a a^2 H\sin^4\theta + O(H^2) \tag{2.15}$$

On the other hand, from the Helfrich constitutive relation[52,53] one can derive[42,51,54,55]

$$B = B_0 + 4k_s H \tag{2.16}$$

$$B_0 = -4k_c H_0, \qquad k_s = k_c + (1/2)\bar{k}_c \tag{2.17}$$

where B_0 is the bending moment for a flat interface ($H = 0$), H_0 is the so-called spontaneous curvature, and k_s is a compound bending elasticity (elastic modulus) for a

(49) Ono, S.; Kondo, S. In *Handbook of Physics*; Flügge, S., Ed.; Springer: Berlin, 1960; Vol. 10, p 134.
(50) Gurkov, T. D.; Kralchevsky, P. A. *Colloids Surf.* **1990**, *47*, 45.
(51) Kralchevsky, P. A.; Eriksson J. C.; Ljunggren, S. *Adv. Colloid Interface Sci.* **1994**, *48*, 19.
(52) Helfrich, W. *Z. Naturforsch.* **1973**, *28c*, 693.
(53) Helfrich, W. *Z. Naturforsch.* **1974**, *29c*, 510.
(54) Ljunggren, S.; Eriksson, J. C.; Kralchevsky, P. A. *J. Colloid Interface Sci.* **1993**, *161*, 133.
(55) Kralchevsky, P. A.; Gurkov, T. D.; Nagayama, K. *J. Colloid Interface Sci.* **1996**, *180*, 619.

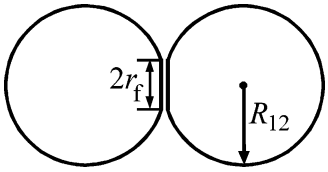

Figure 3. Deformation of two colliding emulsion drops in the zone of their contact. Flattening in the contact zone takes place; r_f is the radius of the formed emulsion film.

spherical interface, which is related to the conventional bending and torsion elastic moduli, k_c and $\bar{k}_c$; see eq 2.17. The comparison of eqs 2.15 and 2.16 yields

$$B_0 = 0 \qquad k_s = \frac{3}{8}\sigma_{12}\varphi_a a^2 \sin^4\theta \tag{2.18}$$

Hence, for the considered case, the bending moment of a planar interface (due to the particles), B_0, and the respective spontaneous curvature, H_0, are equal to zero. The Tolman length (see, e.g., refs 42, 51, and 55), $\delta_0 = B_0/(2\sigma_{12})$, is also zero. On the other hand, there is a nonzero bending elasticity (rigidity), k_s, which opposes the bending of the interface in both directions (but favors the flattening, see Figure 3). Indeed, the term with ϵ^2 in eq 2.14 is positive, and consequently, every increase of $|\epsilon|$ will increase W, which will be energetically unfavorable. Equation 2.18 shows that k_s is proportional to the area fraction of the adsorbed particles, φ_a, which reflects the fact that (by definition) k_s is due to the adsorbed particles. In particular, for $\varphi_a = 0$ eq 2.18 gives $k_s = 0$. Moreover, eq 2.18 indicates that $k_s \propto a^2$, which is in agreement with the numerical results by Aveyard et al.;[4] see their Figure 25.

Taking some typical parameter values, $\sigma_{12} = 30$ mN/m, $a = 50$ nm, $\varphi_a = 0.7$, and $\sin\theta = 1$, from eq 2.18 we estimate $k_s \approx 2.0 \times 10^{-17}$ J $\approx (4.8 \times 10^3)kT$. The obtained value is about 100 times greater than the experimental bending elasticity of phospholipid bilayers (membranes), $k_c = 1.8 \times 10^{-19}$ J.[56] The latter value could be obtained from eq 2.18 if the particle radius were $a = 4.8$ nm, the other parameters being the same.

2.3. Work of Interfacial Deformation. Since the effect of k_s opposes the interfacial bending (deviation from flat interface), it will favor the flattening of the contact zone between two drops upon collision (Figure 3) and will facilitate flocculation, i.e., formation of aggregates from attached drops. Despite the fact that k_s gives a second-order contribution, $\propto\epsilon^2$, in W, its effect on the interaction between colliding emulsion drops could be essential. Before the collision, the two drops have been spherical ($\epsilon \neq 0$), whereas after the collision, a plane-parallel (with $\epsilon = 0$) film of area πr_f^2 is formed; r_f is the film radius (Figure 3). Correspondingly, in eq 2.14 we have to set $A = 2\pi r_f^2$ (the multiplier 2 accounts for the two film surfaces) and define the work of *bending* (flexural) deformation as[57]

$$\Delta W_b = W(\epsilon{=}0) - W(\epsilon) \tag{2.19}$$

Thus, with the help of eq 2.14, we obtain

$$\Delta W_b = -\frac{3}{2}\pi\sigma_{12} r_f^2 \epsilon^2 \sin^4\theta + O(\epsilon^3) \tag{2.20}$$

For estimates, we take $\theta = 90°$, $\sigma_{12} = 30$ mN/m, and $r_f/R_{12} = 0.05$; note that $r_f^2\epsilon^2 = (r_f/R_{12})^2 a^2$. Using the latter values, together with $kT = 4.1 \times 10^{-21}$ J (room temperature),

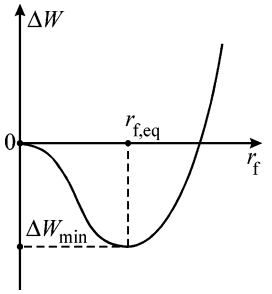

Figure 4. Energy of interfacial deformation, ΔW, versus film radius, r_f: schematic presentation of the dependence given by eq 2.22. $\Delta W_{min} = \Delta W(r_{f,eq})$ corresponds to the formation of an equilibrium doublet of two emulsion drops; see Figure 3.

from eq 2.20 we calculate $8.6kT < |\Delta W_b| < (2.1 \times 10^4)kT$ for particles of radii $10 < a < 500$ nm. Hence, it seems that the bending energy, alone, is large enough to cause the formation of stable flocs of attached emulsion drops, which could not be disrupted by the thermal motion.

Note, however, that the deformation of the emulsion drops upon collision (Figure 3) causes also a dilatation of the oil−water interface, insofar as, at fixed volume, the sphere (the nondeformed drop) has the minimum surface area. The respective work of interfacial *dilatation*, ΔW_{dil}, has been estimated to be[58]

$$\Delta W_{dil} = \sigma_{12} R_{12}^2 \left[\frac{\pi}{2}\frac{r_f^4}{R_{12}^4} + O\left(\frac{r_f^8}{R_{12}^8}\right)\right] \tag{2.21}$$

ΔW_{dil} is positive and causes repulsion between the two colliding drops. In eq 2.21, the surface dilatational (Gibbs) elasticity gives a contribution of higher order, which is usually negligible.[42,58] The total work of interfacial deformation is

$$\Delta W = \Delta W_b + \Delta W_{dil} \approx -2\pi\sigma_{12} r_f^2 \epsilon^2 \sin^4\theta + \frac{\pi}{2}\sigma_{12}\frac{r_f^4}{R_{12}^2} \tag{2.22}$$

In a first approximation (formation of a film of small radius, r_f, between the two drops) we can consider ΔW as a function of r_f at fixed values of all other parameters. The respective dependence $\Delta W(r_f)$, given by eq 2.22, exhibits a minimum, as shown schematically in Figure 4. The radius, $r_{f,eq}$, of the equilibrium film between two attached drops (Figure 4) corresponds to the minimum of ΔW with respect to r_f

$$\left.\frac{\partial(\Delta W)}{\partial r_f}\right|_{r_f = r_{f,eq}} = 0 \tag{2.23}$$

When differentiating eq 2.22 in accordance with eq 2.23, R_{12} (and ϵ) must be kept constant, because in this case R_{12} is a characteristic of the initial state of spherical drop, cf. eq 2.19, rather than a variable of deformation. (Mathematically, R_{12} enters the expressions of question through the coefficients in the series expansion for $r_f/R_{12} \ll 1$; these coefficients must be calculated for the nondeformed state, corresponding to spherical drops, $r_f = 0$.) Thus, substituting eq 2.22 into eq 2.23, we obtain

$$r_{f,eq} = 2^{1/2} a \sin^2\theta \tag{2.24}$$

Hence, it turns out that the maximum equilibrium film

(56) Evans, E. A. *Biophys. J.* **1983**, *43*, 27.
(57) Petsev, D. N.; Denkov, N. D.; Kralchevsky, P. A. *J. Colloid Interface Sci.* **1995**, *176*, 201.
(58) Danov, K. D.; Petsev, D. N.; Denkov, N. D., Borwankar, R. *J. Chem. Phys.* **1993**, *99*, 7179.

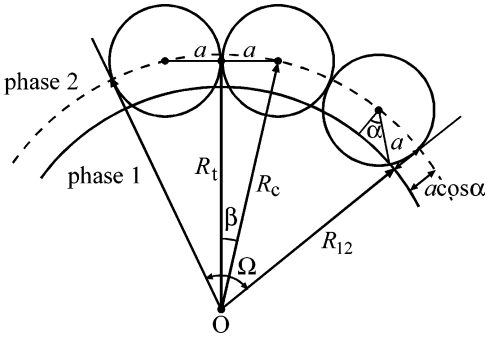

Figure 5. Sketch of a layer of closely packed spherical particles at the surface of an emulsion drop from phase 1 surrounded by phase 2. The notations are explained in the text.

radius, $r_{f,eq}$, that for $\theta \approx 90°$, is of the order of the particle radius, a. In other words, a very small equilibrium film is formed, which contains only one to two particles at its surfaces. In such a case, we could not speak about the appearance of a real plane-parallel film between two colliding drops and about the occurrence of a real flocculation.

In conclusion, in the considered case of non-closely-packed particle monolayer, the bending energy leads to an effective attraction between two colliding emulsion drops (eq 2.20), which is, however, unable to produce flocculation in the Pickering emulsions because of the predominant repulsive effect of the interfacial dilatation, ΔW_{dil}, given by eq 2.21.

3. Bending of a Closely Packed Particle Monolayer

3.1. Expression for the Bending Energy. Some attractive interactions, like the van der Waals forces[59] and the electric-field-induced capillary force,[21,24] may push the particles to stay in close contact with each other. Thus, the particles will be always in contact, both at rest and during an interfacial deformation. In such a case, the interfacial bending will be accompanied by a dilatation or shrinking of the oil−water interface. This case was discussed by Aveyard et al.;[35] see their Figure 15. Our aim here is to continue their analysis by deriving explicit expressions for the bending moment (B_0), for the bending elasticity (k_s), and for the work of bending upon collision of two drops (ΔW_b) and, finally, to compare the latter with the work of dilatation, ΔW_{dil}.

Let us consider a parcel of a spherical oil−water interface, which contains a *fixed* number of closely packed particles, N_p. The last term in eq 2.4 is constant again, so it is sufficient to consider the following reduced expression for the interfacial energy

$$\tilde{W} = \sigma_{12}\left[\Omega R_{12}^{\,2} - N_p \pi a^2\left(\sin^2\alpha + \frac{1}{4}\epsilon^2 \sin^4\alpha\right)\right] - 2\pi a^2 N_p \sigma_{12} \cos\theta \cos\alpha \quad (3.1)$$

where eq 2.8 was used with $A = \Omega R_{12}^{\,2}$ being the area of the oil−water interface, corresponding to the considered parcel and Ω is the respective body angle; see Figure 5. The body angle, corresponding to a single particle, is $2\pi(1 - \cos\beta)$, where the angle β is also shown in Figure 5. Note that

$$\sin\beta = a/R_c; \qquad R_c = R_{12} + a\cos\alpha \quad (3.2)$$

R_c is the radius of the sphere passing through the centers of the adsorbed particles. Furthermore, if R_t is the radius of the sphere passing through the points of contact of the neighboring particles, then the number of particles, N_p, will be equal to the total area $\Omega R_t^{\,2}$ divided by the area per particle

$$N_p = \frac{\Omega R_t^{\,2}}{2\pi R_t^{\,2}(1 - \cos\beta)\lambda^{-1}}, \qquad \lambda = \frac{\pi}{2(3^{1/2})} \quad (3.3)$$

Here $\lambda \approx 0.907$ accounts for the area fraction of the particles in a closely packed monolayer. Note that $2\pi R_t^{\,2}\cdot(1 - \cos\beta)$ is the area of the spherical segment occupied by a single particle, while the multiplier λ^{-1} in the denominator of eq 3.3 accounts for the greater area of the hexagon described around this circular segment. Since $\sin\beta = a/R_c$ is a small quantity, we have

$$1 - \cos\beta = 1 - (1 - \eta^2)^{1/2} = (1/2)\eta^2(1 + (1/4)\eta^2 + ...) \quad (3.4)$$

where $\eta = a/R_c$. R_t disappears from eq 3.3, and $1 - \cos\beta$ can be substituted from eq 3.4; thus from eq 3.3 we obtain

$$\Omega R_c^{\,2} = \pi a^2 \lambda^{-1} N_p (1 + (1/4)\eta^2 + ...) \quad (3.5)$$

In addition, we have $R_c = R_{12}(1 + \epsilon\cos\alpha)$, where, as usual, $\epsilon = a/R_{12}$. We substitute the latter expression for R_c in eq 3.5 and expand in series with respect to ϵ

$$\Omega R_{12}^{\,2} = \pi a^2 \lambda^{-1} N_p [1 - 2\epsilon\cos\alpha + \epsilon^2((1/4) + 3\cos^2\alpha) + ...] \quad (3.6)$$

Further, we substitute eq 3.6 into eq 3.1

$$\frac{\tilde{W}}{\tilde{A}} = \sigma_{12}[1 - 2\epsilon\cos\alpha + \epsilon^2((1/4) + 3\cos^2\alpha) - \lambda(\sin^2\alpha + (1/4)\epsilon^2\sin^4\alpha + 2\cos\theta\cos\alpha)] \quad (3.7)$$

where $\tilde{A} = N_p \pi a^2 \lambda^{-1}$ is the area occupied by the closely packed particles. Next, in eq 3.7 we replace $\cos\alpha$ from eq 2.13 and bring the result in the form of an expansion with respect to the powers of ϵ

$$\frac{\tilde{W}}{\tilde{A}} = \sigma_{12}\left[1 - \lambda(1 + \cos^2\theta) - 2\epsilon\cos\theta + \epsilon^2\left(\frac{3}{4}\lambda\sin^4\theta + 5\cos^2\theta - \frac{7}{4}\right) + O(\epsilon^3)\right] \quad (3.8)$$

($\epsilon \ll 1$). In analogy with eq 2.10, the bending moment can be calculated from the expression

$$B = \left(\frac{\partial(\tilde{W}/\tilde{A})}{\partial H}\right)_{\tilde{A}} \quad (3.9)$$

Having in mind that $\epsilon = -aH$, we differentiate eq 3.8, in accordance with eq 3.9

$$B = 2\sigma_{12}a\cos\theta + 2H\sigma_{12}a^2\left(\frac{3}{4}\lambda\sin^4\theta + 5\cos^2\theta - \frac{7}{8}\right) \quad (3.10)$$

The comparison of eq 3.10 with eq 2.16 yields

$$B_0 = 2\sigma_{12}a\cos\theta \quad (3.11)$$

(59) Israelachvili, J. N. *Intermolecular and Surface Forces*; Academic Press: London, 1992.

$$k_s = \frac{1}{2}\sigma_{12}a^2\left(\frac{3}{4}\lambda \sin^4\theta + 5\cos^2\theta - \frac{7}{8}\right) \quad (3.12)$$

Correspondingly, the Tolman length is $\delta_0 = B_0/(2\sigma_{12}) = a\cos\theta$. Note that, in fact, δ_0 is the distance between the contact point of two neighboring particles and the oil−water interface (Figure 5; $\alpha \approx \theta$). Hence, in terms of the Gibbs interfacial thermodynamics, the sphere passing through the particle contact points serves as the *surface of tension*, while the oil−water interface (of radius R_{12}) can be identified as the *equimolecular dividing surface*.[49] On the other hand, from the viewpoint of the interfacial mechanics,[50,51] B_0 is the trace of the tensor of the surface moments (torques). Thus, for a spherical interface $B_0 = 2M$, where the surface moment, M, can be identified with a force couple of arm δ_0. The two forces in the couple have magnitude σ_{12}; the lower force is the oil−water interfacial tension exerted at the contact line, while the upper one is the bearing reaction at the point of contact of two neighboring particles. Thus, $M = \sigma_{12}a\cos\theta$, and we arrive again at eq 3.11.

For $\theta < 90°$, the bending moment of the flat interface, B_0, is positive, which means that it will oppose the flattening in the zone of contact upon collision of two emulsion drops; this is a stabilizing effect. In contrast, for $\theta > 90°$, B_0 is negative, which has a destabilizing effect on the emulsions; see section 3.2 for details. As a numerical example, we substitute $\theta = 60°$, $\sigma_{12} = 30$ mN/m, and $a = 50$ nm in eq 3.11 and obtain $B_0 = 1.5 \times 10^{-4}$ dyn, which is about 30 times greater than the bending moments of fluid interfaces without particles.[42,55,60] Moreover, eq 3.11 shows that B_0 grows linearly with the particle radius, a. Because the contribution of k_s is a higher order effect ($\propto\epsilon^2$ in $\tilde{W}$, eq 3.8), it is usually negligible in comparison with the contribution of B_0, except for $\theta = 90°$, for which $B_0 = 0$; see eq 3.11.

3.2. Work of Interfacial Deformation. As in section 2.3, here we consider the deformation in the contact zone of two colliding emulsion droplets (Figure 3). During the deformation, work of dilatation and bending, $\Delta W_{dil} + \Delta W_b$, is carried out. ΔW_{dil} is given again by eq 2.21, while the expression for ΔW_b can be obtained by substituting eq 3.8 into eq 2.19 (the latter with $\tilde{W}$ instead of W). The result reads

$$\Delta W_b = 2\pi r_f^2 B_0/R_{12} = 4\pi\sigma_{12}r_f^2\epsilon\cos\theta \quad (3.13)$$

where the terms of order ϵ^2 (see eq 3.8) have been neglected and B_0 is given by eq 3.11. Combining eqs 2.21 and 3.13, we obtain an expression for the work of interfacial deformation in the considered case of a closely packed particle monolayer

$$\Delta W = \Delta W_b + \Delta W_{dil} \approx 4\pi\sigma_{12}r_f^2\epsilon\cos\theta + \frac{\pi}{2}\sigma_{12}\frac{r_f^4}{R_{12}^2} \quad (3.14)$$

Below we consider separately the cases $\theta < 90°$ and $\theta > 90°$.

In the case $\theta < 90°$, both ΔW_b and ΔW_{dil} are positive and lead to repulsion between the two colliding drops (Figure 3). In Figure 6a, we illustrate the relative importance of the contributions of ΔW_b and ΔW_{dil} into ΔW. For this purpose, ΔW, ΔW_b, and ΔW_{dil} are plotted versus r_f/a, which characterizes the magnitude of deformation of the two

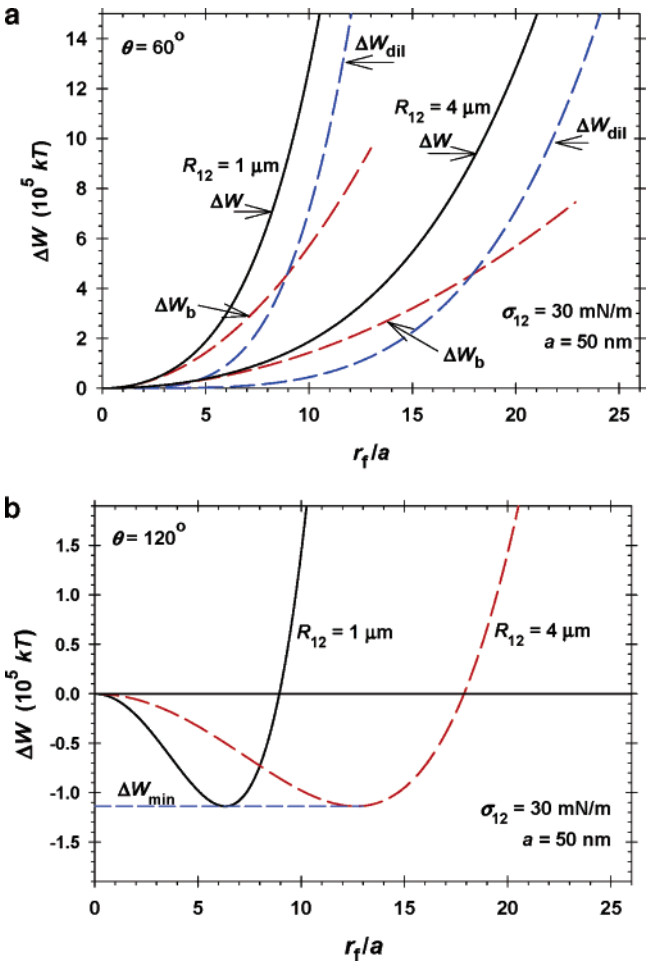

Figure 6. Energy of interfacial deformation, $\Delta W = \Delta W_b + \Delta W_{dil}$, plotted vs the film radius, r_f, scaled by the particle radius, a. ΔW_b and ΔW_{dil} are the works of bending and dilatational deformations, respectively. The curves are calculated from eq 3.14 for $a = 50$ nm, $\sigma_{12} = 30$ mN/m, for two-drop radii: $R_{12} = 1$ and 4 μm; (a) $\theta = 60°$, (b) $\theta = 120°$.

drops. Typical parameter values are used: $\sigma_{12} = 30$ mN/m; $a = 50$ nm; $\theta = 60°$; $R_{12} = 1$ and 4 μm. As $\Delta W_b \propto r_f^2$, it dominates ΔW for small deformations (small r_f). On the other hand, because $\Delta W_{dil} \propto r_f^4$ it dominates ΔW for relatively larger deformations. The transition between the two regimes can be characterized by the value of r_f, for which $\Delta W_b = \Delta W_{dil}$. From eq 3.14 we determine that the respective value is $r_f^* = (8aR_{12}\cos\theta)^{1/2}$. Thus for the two drop sizes in Figure 6a, we determine $r_f^* \approx 9a$ and $18a$. In general, it turns out that the bending energy, ΔW_b (as well as the dilatational energy, ΔW_{dil}), could have a significant stabilizing effect on Pickering emulsions, supposedly the particle monolayer is closely packed and $\theta < 90°$.

In the case of $\theta > 90°$, eqs 2.21 and 3.13 imply that $\Delta W_{dil} > 0$, whereas $\Delta W_b < 0$. In such a case, the dependence $\Delta W(r_f)$ exhibits a minimum that corresponds to the formation of an equilibrium doublet of two attached emulsion drops (Figure 3). In other words, one could expect the appearance of spontaneous flocculation in such emulsions. In Figure 6b we illustrate the dependence $\Delta W(r_f)$ for the same parameter values, as in Figure 6a, with the only difference that now $\theta = 120°$. From eq 3.14, we determine that the minimum of $\Delta W(r_f)$ corresponds to

$$r_{f,eq} = 2(aR_{12}|\cos\theta|)^{1/2} \quad (\theta > 90°) \quad (3.15)$$

(60) Gurkov, T. D.; Kralchevsky, P. A.; Ivanov, I. B. *Colloids Surf.* **1991**, *56*, 119.

$$\Delta W_{\min} \equiv \Delta W(r_{f,eq}) = -8\pi\sigma_{12}a^2 \cos^2\theta \quad (3.16)$$

It is interesting to note that $\Delta W_{\min}$ is determined by the particle radius a, and the contact angle, θ, but is independent of the drop radius, R_{12}. Thus for the two curves in Figure 6b, corresponding to $R_{12} = 1$ and 4 μm, we have the same $\Delta W_{\min} = (1.1 \times 10^5)kT$, while $r_{f,eq}/a = 6.3$ and 12.6, respectively; i.e., $r_{f,eq}$ is greater for the bigger drops. The depth of the minimum, $\Delta W_{\min}$, turns out to be considerable, and consequently, the thermal motion is unable to disrupt the equilibrium doublets of emulsion drops. As a result, for $\theta > 90°$ one should observe flocculation and creaming in the respective emulsions.

3.3. Particle Bridging Effect and Drop Coalescence. As demonstrated in section 3.2, the bending energy, ΔW_b, certainly has an important effect on the Pickering emulsions, which could be either stabilizing of destabilizing depending on whether $\theta < 90°$ or $\theta > 90°$. In addition, it should be noted that the effect of bending energy could appear in interplay with the particle bridging effect. The role of the latter is briefly discussed below.

In the collision zone between two emulsion drops, it may happen that one particle is adsorbed simultaneously at the two film surfaces (Figure 7).[26,28,29] Such a particle keeps the two oil−water interfaces at a distance

$$h = 2a \cos\theta \quad (3.17)$$

For $\theta = 90°$, eq 3.17 yields $h = 0$, which means that the particle will bring the two oil−water interfaces into contact and will cause coalescence of the two emulsion droplets. The same will happen if $\theta > 90°$. A similar bridging-dewetting phenomenon is observed when hydrophobic particles are used to destroy foams.[61,62] (Although qualitatively similar, the real situation with a bridging particle is more complicated than that depicted in Figure 7: because the pressure inside the drops is higher than that in the outer phase, curved menisci are formed around the particle; analysis of this more complicated case can be found in refs 29 and 30.)

In summary, the result of particle bridging is different for $\theta < 90°$ and $\theta > 90°$. In the former case, the bridging particle has a stable position, like that in Figure 7. In this case, the particles serve as adhesives for the emulsion drops and are able to produce *flocculation*. In contrast, for $\theta > 90°$ the bridging particles serve as a connection, which brings the two oil−water interfaces into a close contact and produces *coalescence* of the two drops.

The above considerations imply the following possible picture and mechanism of drop coalescence for $\theta > 90°$. (i) The collision of two droplets leads to the spontaneous formation of a doublet of two drops (Figure 3) due to the effect of bending energy; see the minimum in Figure 6b. (ii) The local dilatation of the interface in the zone of contact favors the appearance of bridging particles, which cause coalescence of the two drops.

In contrast, for $\theta < 90°$ the bending energy produces a stabilizing effect (Figure 6a), the oil drops are protected against deformation upon collision, and local dilatation of the oil−water interface is prevented. In such a case, the appearance of bridging particles is impossible (supposedly the adsorption monolayer is closely packed) and the emulsion remains stable.

Of course, the above conclusions are valid for the case of dense particle monolayers on the drop surfaces. However, if the particle monolayer is not dense, then we have $B_0 = 0$, the effect of bending energy is practically negligible (section 2.3), while the bridging effect will be enhanced, insofar as there would be larger free spaces among the adsorbed particles (greater probability for bridging). In such a case, the emulsion stability will be governed by the bridging effect, which will produce either drop flocculation (for $\theta < 90°$) or drop coalescence (for $\theta \geq 90°$).

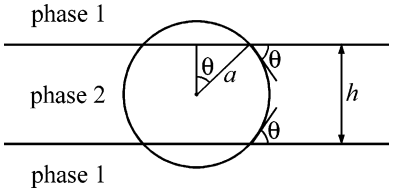

Figure 7. Sketch of a particle of radius a, which is bridging between the surfaces of a film from phase 2 formed between two drops of phase 1. h is the film thickness. θ is the contact angle.

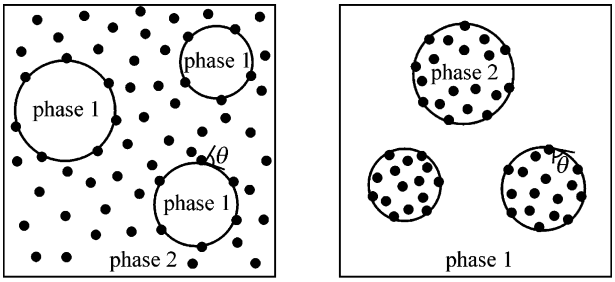

Figure 8. Definitions of phases, angles, and emulsions: By definition, the particles are initially dispersed in phase 2. The contact angle, θ, is always measured across phase 2. The emulsion 1-in-2 is a Bancroft-type emulsion, in which the particles are dispersed in the continuous phase. In contrast, the emulsion 2-in-1 is of anti-Bancroft type.

4. Work of Emulsification

4.1. General Expressions. Unlike the spontaneously forming microemulsions, the formation of Pickering emulsions demands an input of mechanical work. It is needed to break the disperse phase down to small drops. Next, the solid particles adsorb on the newly formed oil−water interface, which is accompanied by a gain of adsorption energy. The produced emulsion can be very stable owing to the steric drop−drop repulsion provided by the adsorbed particles. Such emulsions could have a lifetime of years upon the storage shelf.[4] From a thermodynamic viewpoint, the formed Pickering emulsion corresponds to a metastable state of the system.

Here and hereafter, we assume that the solid particles are initially dispersed in phase 2. For brevity, the dispersion of phase 1 into phase 2 will be termed "emulsion 1-in-2". It corresponds to the Bancroft rule,[63] as the particles are in the continuous phase. The dispersion of phase 2 into phase 1 (reverse to the Bancroft rule) will be called "emulsion 2-in-1"; see Figure 8. For example, if the particles are initially dispersed in the water phase, then the direct emulsion (oil-in-water) will be "emulsion 1-in-2", while the reverse emulsion (water-in-oil) will be "emulsion 2-in-1".

By definition, the contact angle, θ, is measured across the phase 2. In general, we will consider the whole interval $0 < \theta < 180°$. In other words, we do not follow the artificial restriction that the particles be initially dissolved in the

(61) Garrett, P. R. *J. Colloid Interface Sci.* **1979**, *69*, 107.
(62) Garrett, P. R. *J. Colloid Interface Sci.* **1980**, *76*, 587.
(63) Bancroft, W. D. *J. Phys. Chem.* **1913**, *17*, 514.

phase in which $\theta < 90°$, because it does not cover all possible experimental situations. For example, the experiment shows that polystyrene latex particles, which are usually dispersed in the water phase, have a contact angle $\theta \approx 130°$ (across water).[26,28]

The breakage of a given volume of liquid to droplets (of decreasing size and increasing number) leads to enlargement of the surface area and to adsorption of additional solid particles. The volumes of phases 1 and 2, V_1 and V_2, as well as the total number of particles are assumed to be constant during emulsification

$$N_a + N_b = \text{constant} \tag{4.1}$$

Here N_a is the total number of particles that are adsorbed at the drop surfaces, while N_b is the total number of (nonadsorbed) particles in the bulk of the liquid phase 2. Note that, in contrast with sections 2 and 3, here the number of adsorbed particles is not constant. Indeed, N_a will grow if phase 1 (or 2) is broken to droplets of decreasing size and increasing number.

For simplicity, we assume that the emulsion drops are monodisperse and N_p particles are adsorbed on each drop. Thus, we have

$$N_a = N_d N_p \tag{4.2}$$

where N_d is the total number of drops. The interfacial work of emulsification is

$$W = \sigma_{12}A_{12} + \sigma_{1p}A_{1p} + \sigma_{2p}A_{2p} + N_b\sigma_{2p}4\pi a^2 \tag{4.3}$$

The last term in eq 4.3 accounts for the interfacial energy of the particles, which remain dispersed in the bulk of phase 2. The interfacial areas in eq 4.3 are

$$A_{12} = N_d\left[4\pi R_{12}^2 - N_p\pi a^2\left(\sin^2\alpha + \frac{\epsilon^2}{4}\sin^4\alpha\right)\right] \tag{4.4}$$

$$A_{1p} = N_a 2\pi a^2(1 - \cos\alpha), \qquad A_{2p} = N_a 2\pi a^2(1 + \cos\alpha) \tag{4.5}$$

where the angle α is shown in Figure 2; see also eq 2.8. Substituting eqs 4.4 and 4.5 into eq 4.3, and using eqs 2.13 and 4.2 and the Young equation, $\sigma_{1p} - \sigma_{2p} = \sigma_{12}\cos\theta$, we obtain

$$W = 4\pi R_{12}^2\sigma_{12}N_d - N_a\pi a^2\sigma_{12}[(1 - \cos\theta)^2 + O(\epsilon^2)] + 4\pi a^2\sigma_{2p}(N_a + N_b) \tag{4.6}$$

The first term in eq 4.6 corresponds to the interfacial energy of the bare drops (without adsorbed particles). The term $\propto(1 - \cos\theta)^2$ accounts for the decrease in the interfacial energy owing to the adsorption of solid particles at the drop surfaces.[29,64] Finally, in accordance with eq 4.1, the last term in eq 4.6 is constant and can be omitted. Next, we consider separately the cases of emulsions 1-in-2 and 2-in-1.

4.2. Emulsion 1-in-2: Work of Formation. For the emulsion 1-in-2, the *continuous* phase is phase 2, which contains the particles. For such an emulsion, eq 2.13 gives

$$\cos\alpha = \cos\theta + \epsilon\sin^2\theta + O(\epsilon^2) \tag{4.7}$$

where, as usual, $\epsilon = a/R_{12}^2$. As we have $N_a = N_d N_p$, eq 4.6 acquires the form

$$W = 4\pi\sigma_{12}R_{12}^2N_d\left\{1 - N_p\frac{a^2}{4R_{12}^2}[(1 - \cos\theta)^2 + O(\epsilon^2)]\right\} \tag{4.8}$$

The number of particles per drop, N_p, can be expressed by using an analogue of eq 3.3, where the body angle is $\Omega = 4\pi$ for the whole drop and the maximum particle area fraction, λ, is replaced by the particle area fraction, φ_a; note that $0 < \varphi_a < \lambda = 0.907$. Thus, eq 3.3 acquires the form

$$N_p = \frac{4\pi}{2\pi(1 - \cos\beta)\varphi_a^{-1}} = \frac{4R_c^2\varphi_a}{a^2}[1 + O(\epsilon^2)] \tag{4.9}$$

where we have used the relationship $\cos\beta = (1 - a^2/R_c^2)^{1/2}$. Substituting $R_c = R_{12} + a\cos\alpha$, and using eq 4.7, we bring eq 4.9 in the form

$$N_p = \frac{4R_{12}^2\varphi_a}{a^2}[1 + 2\epsilon\cos\theta + O(\epsilon^2)] \tag{4.10}$$

The factor before the brackets gives the number of particles for a planar interface. The term $2\epsilon\cos\theta$ in eq 4.10 accounts for the fact that for $\theta < 90°$ more particles can be adsorbed at the surface of a *convex* drop ($\epsilon > 0$), in comparison with a flat interface ($\epsilon = 0$). Next, we take into account the circumstance that the adsorption of each particle displaces some liquid from the drop phase and thus leads to some increase in the drop radius, R_{12}. The volume of the sphere of radius R_{12} can be expressed in the form

$$\frac{4}{3}\pi R_{12}^3 = \frac{4}{3}\pi R_0^3 + N_p\frac{\pi}{3}[a^3 f(\alpha) + R_{12}^3 f(\omega)] \tag{4.11}$$

where the angle ω is the same as before (Figure 2); by definition, $4\pi R_0^3/3$ is the volume of phase 1 contained in the drop; the function f is defined as follows

$$f(\theta) = (1 - \cos\theta)^2(2 + \cos\theta) \tag{4.12}$$

In eq 4.11, $\pi a^3 f(\alpha)/3$ is the volume of the truncated sphere, which represents the portion of the particle immersed in the drop phase. Likewise, $\pi R_{12}^3 f(\omega)/3$ is a relatively small term, expressing the volume of another truncated sphere, which is confined between the sphere of radius R_{12} and the plane of the contact line of radius r_c; see Figure 2. After estimating the latter effect, we bring eq 4.11 into the form

$$R_{12}^3 = R_0^3 + \frac{1}{4}N_p a^3[f(\alpha) + 3\epsilon\sin^4\theta + O(\epsilon^2)] \tag{4.13}$$

Next, we substitute N_p from eq 4.10 into eq 4.13 and after some transformations, we get

$$R_0^3 = R_{12}^3[1 - \epsilon\varphi_a f(\theta) + O(\epsilon^2)] \tag{4.14}$$

Then the number of drops can be expressed in the form

$$N_d = \frac{V_1}{(4/3)\pi R_0^3} = \frac{3V_1}{4\pi R_{12}^3}[1 + \epsilon\varphi_a f(\theta) + O(\epsilon^2)] \tag{4.15}$$

where, as usual, V_1 is the total volume of phase 1 in the considered emulsion. Finally, we substitute N_p and N_d

(64) Tadros, Th. V.; Vincent, B. In *Encyclopedia of Emulsion Technology*; Becher, P., Ed.; Marcel Dekker: New York, 1983; Vol. 1, p 129.

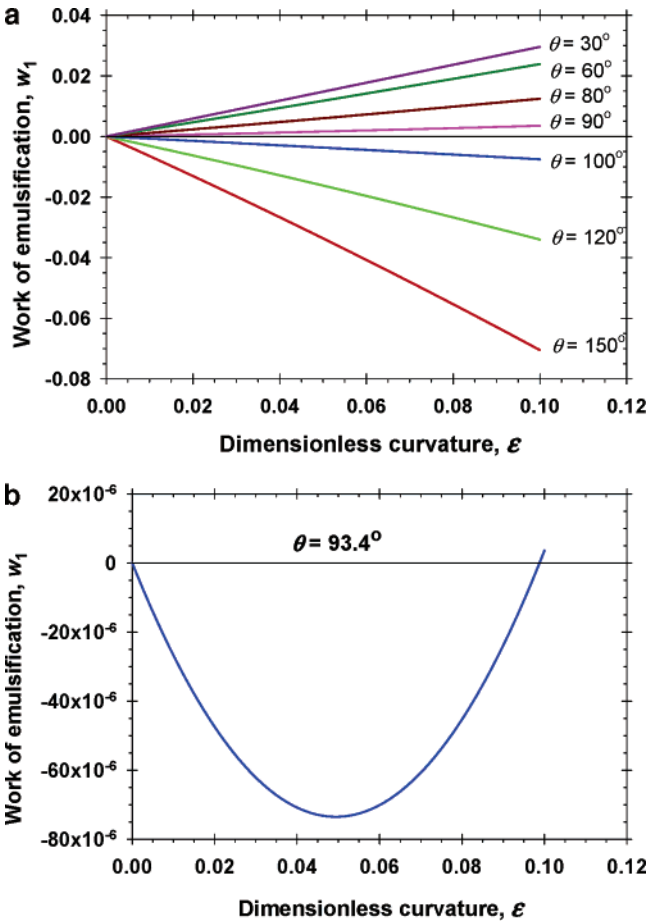

Figure 9. (a) Plot of the dimensionless work for formation of the emulsion 1-in-2, w_1, vs the dimensionless curvature, $\epsilon = a/R_{12}$, at $\varphi_1 = 0.3$ and $\varphi_a = 0.9$. The different curves correspond to different values of the contact angles, θ. (b) The curve for $\theta = 93.4°$ is shown in an enlarged scale to visualize that it has a minimum, corresponding to spontaneous formation of drops with the respective size.

from eqs 4.10 and 4.15 into eq 4.8. After some transformations, we obtain the following expression for the work, W_1, of formation of the emulsion 1-in-2

$$W_1 = \frac{3\sigma_{12}V}{a} w_1 \tag{4.16}$$

$$w_1 = \varphi_1\{\epsilon(1 - \varphi_a b) + \epsilon^2\varphi_a[f(\theta)(1 - \varphi_a b) - 2b\cos\theta] + O(\epsilon^3)\} \tag{4.17}$$

$$b = (1 - \cos\theta)^2, \qquad \varphi_1 = V_1/V \tag{4.18}$$

where w_1 is the respective dimensionless work of emulsification, φ_1 is the volume fraction of phase 1 in the emulsion, and as usual, $\epsilon = a/R_{12}$. Because $\epsilon \ll 1$, the leading term in eq 4.17 is $\varphi_1\epsilon(1 - \varphi_a b)$, which accounts for the formation of new oil−water interface and for the particle adsorption. The curvature effects ($\propto\epsilon^2$) give a higher order contribution, which could be significant only if $(1 - \varphi_a b) \ll 1$. The latter may happen for θ close to 90°.

As an illustration, in Figure 9a we show calculated curves of w_1 vs the dimensionless drop curvature, ϵ, for $0 \le \epsilon \le 0.1$. The other parameters are $\varphi_1 = 0.3$ (bulk volume fraction of the disperse phase) and $\varphi_a = 0.9$ (surface area fraction of the particles). The different curves in Figure 9a correspond to different values of the contact angle θ. Larger ϵ means that phase 1 is dispersed to smaller

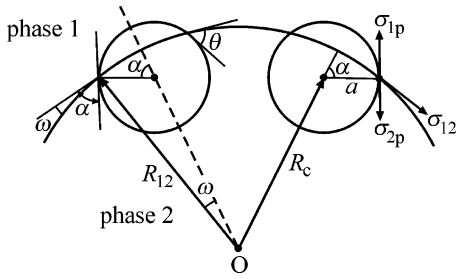

Figure 10. Particles at the surface of a drop in the emulsion 2-in-1 (emulsion 1-in-2 corresponding to Figure 2).

drops. One sees that for $\theta \le 90°$ we obtain $w_1 > 0$, which indicates that an input of mechanical energy is needed to break phase 1 to small drops. In contrast, for $\theta \ge 100°$ we obtain $w_1 < 0$, which means that the emulsion could form spontaneously (in the absence of kinetic barriers). The latter is due to the significant gain of surface energy upon adsorption of particles with $\theta > 90°$. Note, however, that despite the relationship $w_1 < 0$, the reverse emulsion (that is emulsion 2-in-1) is energetically more favorable to form at $\theta > 90°$ and $\varphi_1 < 0.5$; see sections 5.1 and 5.2 below.

Note also that the calculated dependencies $w_1(\epsilon)$ are practically straight lines (Figure 9a). As mentioned above, this is because the linear term ($\propto\epsilon$) is predominant in eq 4.17. Only for $\theta \approx 93°$ is the linear tem small and becomes comparable with the quadratic term ($\propto\epsilon^2$). Then, the dependence $w_1(\epsilon)$ looks like a parabola, which has a minimum for a certain ϵ. This is illustrated in Figure 9b for $\theta \approx 93.4°$; the minimum is at $\epsilon \equiv \epsilon_{sp} \approx 0.05$. Thermodynamically, such a minimum corresponds to a *spontaneous* formation of drops with the respective size. From eq 4.17 we derive the following expressions characterizing the minimum of the dependence $w_1(\epsilon)$

$$\epsilon_{sp} = -\frac{1 - \varphi_a b}{2[f(\theta)(1 - \varphi_a b) - 2b\cos\theta]} \tag{4.19}$$

$$f(\theta)(1 - \varphi_a b) - 2b\cos\theta > 0 \tag{4.20}$$

$$1 - \varphi_a b < 0$$

For $\sigma_{12} = 30$ mN/m and $a = 50$ nm, the depth of the minimum in Figure 9b is $(3\sigma_{12}/a)w_{1,min} \approx 1.3 \times 10^{-4}$ J/cm^3. Note, however, that such a minimum exists only for a very narrow range of values of the contact angle, θ, and it is not clear whether this situation (with spontaneous formation of a monodisperse emulsion) could be realized experimentally. The above considerations, illustrated in Figure 9b, indicate only that such a possibility exists in principle.

4.3. Emulsion 2-in-1: Work of Formation. For the emulsion 2-in-1, by definition, the *disperse* phase is phase 2 (that contains the particles). The contact angle θ is defined in the same way as for the emulsion 1-in-2: θ is measured across phase 2. In contrast, the angle α is defined as shown in Figure 10. Then, instead of eq 4.7, we have

$$\cos\alpha = \cos\theta - \epsilon\sin^2\theta + O(\epsilon^2) \tag{4.21}$$

as usual, $\epsilon = a/R_{12}^2$. Equation 4.8 is valid again. Equation 4.9 is also valid, but now $R_c = R_{12} - a\cos\alpha$. Then, instead of eq 4.10, we get

$$N_p = \frac{4R_{12}^2\varphi_a}{a^2}[1 - 2\epsilon\cos\theta + O(\epsilon^2)] \tag{4.22}$$

The volume of the sphere of radius R_{12} can be expressed in the form

$$\frac{4}{3}\pi {R_{12}}^3 = \frac{4}{3}\pi {R_0}^3 + N_p \frac{\pi}{3}[a^3 g(\alpha) + {R_{12}}^3 f(\omega)] \quad (4.23)$$

where $4\pi R_0^3/3$ is the volume of phase 2 contained in the drop; the function f is given by eq 4.12, while the function g is defined as

$$g(\theta) = 4 - f(\theta) = (1 + \cos\theta)^2(2 - \cos\theta) \quad (4.24)$$

The angle ω is the same as before; see Figure 10. Then, with the help of eq 4.22 we can represent eq 4.23 in the form

$${R_0}^3 = {R_{12}}^3[1 - \epsilon\varphi_a g(\theta) + O(\epsilon^2)] \quad (4.25)$$

The number of drops is

$$N_d = \frac{V_2}{(4/3)\pi {R_0}^3} = \frac{3V_2}{4\pi {R_{12}}^3}[1 + \epsilon\varphi_a g(\theta) + O(\epsilon^2)] \quad (4.26)$$

Finally, we substitute N_p and N_d from eqs 4.22 and 4.26 into eq 4.8; after some transformations, we obtain the following expression for the work, W_2, of formation of the emulsion 2-in-1

$$W_2 = \frac{3\sigma_{12}V}{a} w_2 \quad (4.27)$$

$$w_2 = \varphi_2\{\epsilon(1 - \varphi_a b) + \epsilon^2\varphi_a[g(\theta)(1 - \varphi_a b) + 2b\cos\theta] + O(\epsilon^3)\} \quad (4.28)$$

where, as before, $b = (1 - \cos\theta)^2$, $\varphi_2 = 1 - \varphi_1 = V_2/V$ is the volume fraction of phase 2 in the emulsion, and w_2 is the respective dimensionless work of emulsification. Because $\epsilon \ll 1$, the leading term in eq 4.28 (and in eq 4.17, as well) is $\propto\epsilon(1 - \varphi_a b)$, which accounts for the formation of new oil−water interface and particle adsorption. The curvature effects ($\propto\epsilon^2$) again give a higher order contribution.

For illustration, in Figure 11a we show calculated curves of the dimensionless work of emulsification, w_2, vs the dimensionless drop curvature, ϵ, for $0 \le \epsilon \le 0.1$, and for various contact angles, θ. The other parameter values are $\varphi_2 = 0.3$ (bulk volume fraction of the disperse phase) and $\varphi_a = 0.9$ (surface area fraction of the particles). A comparison of the curves in Figures 9a and 11a indicates that they are almost identical. This is not surprising because, as mentioned above, both eq 4.17 and eq 4.28 are dominated by the linear term $\propto\epsilon(1 - \varphi_a b)$, and in both figures, we have set the volume fraction of the *disperse* phase to be 0.3. In eqs 4.17 and 4.28 there is a linear dependence of the emulsification work on the volume fraction of the disperse phase: $w_1 \propto \varphi_1$ and $w_2 \propto \varphi_2$. The latter fact has important thermodynamic implications, which are investigated in section 5 below.

Only for $\theta \approx 93°$ is the linear tem in eq 4.28 small and becomes comparable with the quadratic term ($\propto\epsilon^2$). Then, the dependence $w_2(\epsilon)$ looks like a parabola, which has a maximum for a certain ϵ. This is illustrated in Figure 11b for $\theta \approx 92.9°$; the maximum is at $\epsilon \equiv \epsilon_{cr} = 0.035$. Thermodynamically, this maximum corresponds to a *critical* drop size for the emulsions of phase 2 into phase 1. For $\epsilon < \epsilon_{cr}$, it is thermodynamically favorable for the formed drops to increase in size (by coalescence), whereas for $\epsilon > \epsilon_{cr}$ it is favorable for the drops to be broken to smaller ones. From eq 4.28 we derive the following relationships characterizing the maximum of the dependence $w_2(\epsilon)$

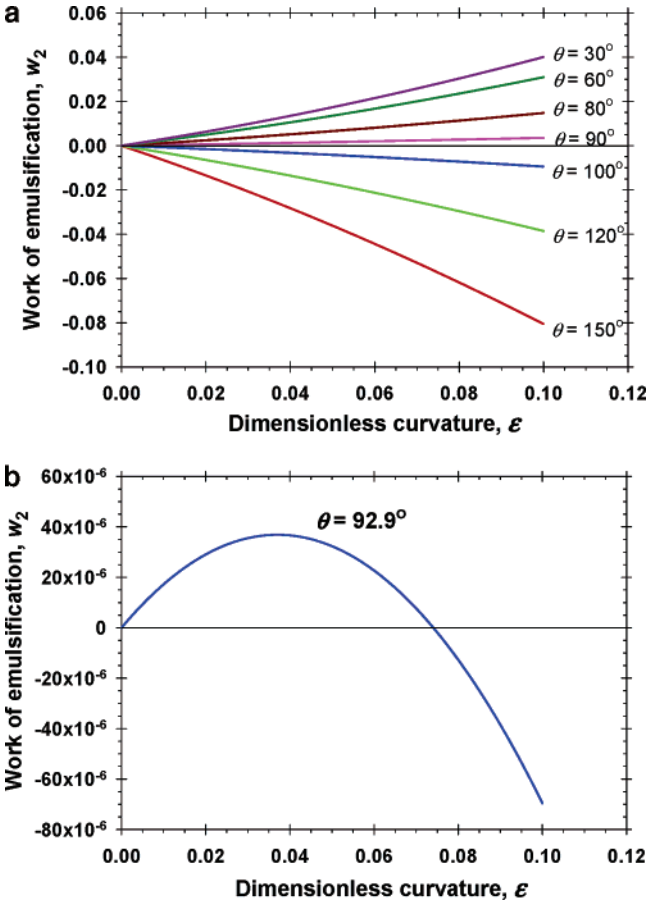

Figure 11. (a) Plot of the dimensionless work for formation of the emulsion 2-in-1, w_2, vs the dimensionless curvature, $\epsilon = a/R_{12}$, at $\varphi_2 = 0.3$ and $\varphi_a = 0.9$. The different curves correspond to different values of the contact angles, θ. (b) The curve for $\theta = 92.9°$ is shown in an enlarged scale to visualize that it has a maximum, corresponding to the critical drop size.

$$\epsilon_{cr} = -\frac{1 - \varphi_a b}{2[g(\theta)(1 - \varphi_a b) + 2b\cos\theta]} \quad (4.29)$$

$$g(\theta)(1 - \varphi_a b) + 2b\cos\theta < 0 \quad (4.30)$$

$$1 - \varphi_a b > 0$$

For $\epsilon > \epsilon_{cr}$ the drop size could spontaneously diminish, while for $\epsilon < \epsilon_{cr}$ an input of external mechanical energy is needed to break the drops. It should be noted that the maximum is present only for a very narrow range of θ values.

5. Thermodynamic Emulsification Criterion

5.1. Type of Emulsion Formed upon Agitation. As mentioned above, our present analysis is purely thermodynamic. In particular, we suppose that the following conditions are fulfilled: (A) the particles adsorb very fast at the oil−water interface; (B) having once adsorbed, the particles do not desorb from the surface of the emulsion drops; (C) the emulsion reaches its thermodynamic equilibrium state of minimal free energy.

It should be noted that kinetic factors (such as high adsorption barriers, low desorption barriers, existence of metastable states, etc.) may lead to violations of the above

conditions and deviations from the predictions of the thermodynamic model. One additional assumption is that the drops are spherical; hence, the volume fraction of the disperse phase cannot be greater than 0.74, corresponding to the close packing of spheres.

According to Davis and Rideal,[65] when a two-phase (oil–water) system is subjected to homogenization, both the direct and reverse emulsions can be simultaneously formed in different spatial domains of the system. However, only that which is more stable survives.[65] From a thermodynamic viewpoint, more stable is the state of lower free energy. In the case of Pickering emulsions, the gain of surface free energy upon particle adsorption is usually much greater than the entropy effects accompanying emulsification.[3,4] For this reason, the difference between the (interfacial) works for formation of the emulsions 1-in-2 and 2-in-1

$$\Delta w = w_1 - w_2 \tag{5.1}$$

provides a thermodynamic *criterion* about which emulsion will form upon agitation

For $\Delta w < 0$, emulsion1-in-2 will form

For $\Delta w > 0$, emulsion 2-in-1 will form (5.2)

w_1 and w_2 are given by eqs 4.17 and 4.28, respectively. Note, that Δw is a dimensionless quantity; the respective dimensional quantity is $\Delta W = (3\sigma_{12}V/a)\Delta w$. Substituting the latter two equations into eq 5.1, we obtain

$$\Delta w = \epsilon\{(\varphi_1 - \varphi_2)(1 - \varphi_a b) + \epsilon\varphi_a[(\varphi_1 f(\theta) - \varphi_2 g(\theta))(1 - \varphi_a b) - 2b\cos\theta]\} \tag{5.3}$$

In the above expression we substitute f and g from eqs 4.12 and 4.24 and take into account that $\varphi_2 = 1 - \varphi_1$

$$\Delta w = \epsilon(2\varphi_1 - 1)(1 - \varphi_a b) + \epsilon^2\varphi_a[((2 + \cos\theta)b + 4\varphi_1 - 4)(1 - \varphi_a b) - 2b\cos\theta] \tag{5.4}$$

where, as before, $b = (1 - \cos\theta)^2$; the term $\propto\epsilon^3$ has been neglected.

Figure 12 shows plots of Δw vs the dimensionless drop curvature, ϵ, for various values of the contact angle θ and for two volume fractions of phase 1: $\varphi_1 = 0.3$ (Figure 12a) and $\varphi_1 = 0.7$ (Figure 12b). For the particles with $\theta \leq 90°$, in Figure 12a we have $\Delta w < 0$ and for them the emulsion 1-in-2 will be formed; see eq 5.2. For the same particles (with $\theta \leq 90°$), in Figure 12b we have $\Delta w > 0$ and then the emulsion 2-in-1 will be formed. This phase inversion happens at volume fractions 50:50, owing to the change in the sign of the leading term in eq 5.3, which is proportional to $(\varphi_1 - \varphi_2)$. In other words, for $\varphi_1 > 0.5$ the formation of the emulsion 2-in-1 becomes more advantageous in terms of interfacial free energy. The latter prediction of the thermodynamic model gives a possible explanation of the catastrophic phase inversion observed with the Pickering emulsions.[17] (For discussion, see section 5.3 below.)

In the special case when $\varphi_1 = \varphi_2 = 0.5$, eq 5.4 simplifies

$$\Delta w = \epsilon^2\varphi_a[((2 + \cos\theta)b - 2)(1 - \varphi_a b) - 2b\cos\theta] \tag{5.5}$$

(65) Davies, J. T.; Rideal, E. K. *Interfacial Phenomena*; Academic Press: New York, 1963.

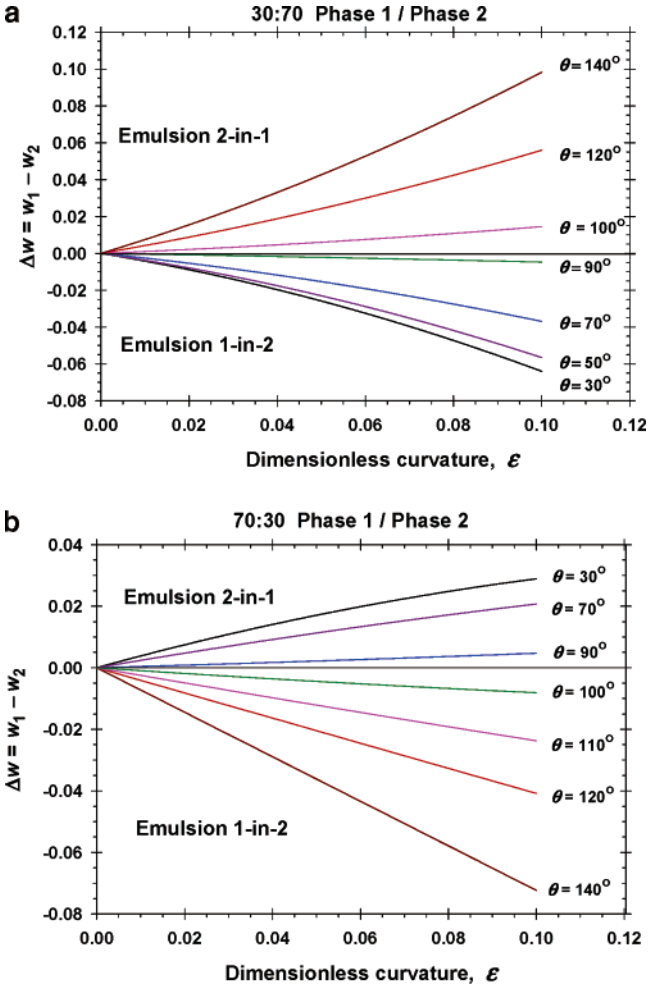

Figure 12. Plot of Δw vs the dimensionless curvature, $\epsilon = a/R_{12}$, of the formed drops: (a) $\varphi_1 = 0.3$; (b) $\varphi_1 = 0.7$. The different curves correspond to different values of the contact angles, θ; $\varphi_a = 0.9$ is fixed. $\Delta w < 0$ and $\Delta w > 0$ correspond to the formation of emulsions 1-in-2 and 2-in-1, respectively.

Equation 5.5 can be expressed in the equivalent form

$$\Delta w = -\epsilon^2\varphi_a x F(x) \qquad (\varphi_1 = \varphi_2 = 0.5) \tag{5.6}$$

$$F(x) = 3 - x^2 + (1 - x)^2[2 - (3 - x^2)\varphi_a] \tag{5.7}$$

where $x = \cos\theta$. As $\varphi_a < 1$, it can be proven that $F(x) > 1$ for $-1 \leq x \leq 1$. For $\theta = 90°$ we have $x = 0$, and eq 5.6 yields $\Delta w = 0$, as it could be expected because of the symmetry of the system. Furthermore, for $\theta < 90°$ eq 5.6 predicts that Δw is always negative, i.e., the formation of the emulsion 1-in-2 is energetically favorable. In contrast, for $\theta > 90°$ we obtain $\Delta w > 0$, and consequently, eq 5.6 implies that the formation of the emulsion 2-in-1 will be advantageous. This conclusion is in agreement with the experimental facts (see Figure 1) and with the predictions based on the bending-energy considerations in section 3.2. Note, however, that the effect of the bending energy is significant only for closely packed particle monolayers, while the conclusions from eq 5.6 are valid for every $0 < \varphi_a < 1$.

We should note that Δw in eq 5.6 and the ϵ^2 term in eqs 4.17, 4.28, and 5.4 expresses an effect of the interfacial curvature, which is different from the work of bending, ΔW_b, considered in sections 2 and 3. Indeed, the term of question originates from the terms $\propto\epsilon$ in the expressions

Table 1. Emulsion Type and Stability vs Volume Fractions and Contact Angle, θ

vol fractions	$\theta \leq 90°$	$\theta > 90°$
$\varphi_1 \leq \varphi_2$ normal emulsion	$\Delta w < 0$ (emulsion 1-in-2) $\Delta W_b > 0$ (stable)	$\Delta w > 0$ (emulsion 2-in-1) $\Delta W_b > 0$ (stable)
$\varphi_1 > \varphi_2$ anomalous emulsion	$\Delta w > 0$ (emulsion 2-in-1) $\Delta W_b < 0$ (flocculated)	$\Delta w < 0$ (emulsion 1-in-2) $\Delta W_b < 0$ (flocculated)

for N_p and N_d; see eqs 4.10 and 4.15. The latter terms account for the following two effects: First, at a fixed particle area fraction on the oil−water interface, φ_a, the surface-to-surface distances between the adsorbed particles (and the total interfacial area accessible to their adsorption) depends on the interfacial curvature. Second, the adsorbed particles displace a part of the inner phase, thus increasing the drop radius and providing some extra area for particle adsorption. These curvature effects ($\propto\epsilon^2$) can significantly influence Δw only at $\varphi_1 = \varphi_2 = 0.5$, when the leading term ($\propto\epsilon^1$) in eq 5.3 is zero.

5.2. Discussion. The results obtained in section 5.1 and illustrated in Figure 12 call for a more detailed discussion and systematization. First, the basis to compare the surface works for emulsification, w_1 and w_2, in eq 5.2 and Figure 12, at the *same* ϵ (at the same drop size), is the following. For a given input of mechanical energy in the system, upon agitation, the diameters of the produced primary drops (before any coalescence) have to be practically the same in the direct and reverse emulsions. For example, the average Kolmogorov diameter, d_K, of the produced drops is determined by the formula for emulsification in turbulent inertial regime[43,44,46]

$$d_K \approx \hat{\epsilon}^{-2/5}\sigma_{ow}^{3/5}\rho_c^{-1/5} \tag{5.8}$$

where $\hat{\epsilon}$ is the input mechanical energy per unit time and per unit volume, σ_{ow} is the oil−water interfacial tension, and ρ_c is the mass density of the continuous phase. Obviously, σ_{ow} and $\hat{\epsilon}$ are the same for the direct and reverse emulsion, $\hat{\epsilon}$ being determined by the design and power of the used emulsification apparatus. Moreover, as the mass densities of the oil and water phases are not so different, the quantity $\rho_c^{-1/5}$ (and d_K as well) will be practically the same for the direct and reverse emulsion.

Furthermore, in Table 1 we have systematized the four major cases with respect to Δw and ΔW_b. In accordance with eq 5.2, we have assumed that the sign of the emulsification work, Δw, determines the type of the formed emulsion (emulsion 1-in-2 or 2-in-1), while the sign of the work of bending, ΔW_b, determines whether the formed emulsion will be stable, or flocculated and unstable; see eq 3.13 and Figure 6. "Unstable" here means that if the emulsion drops exhibit a tendency to flocculate (Figure 6b), this will lead to creaming and, eventually, to drop coalescence. Note also, that Δw does not change sign exactly at $\theta = 90°$ (as denoted approximately in Table 1) but at some angle close to 90°; see Figure 12.

In view of eqs 3.11 and 3.13, we have $\Delta W_b \propto (\cos\theta)/R_{12}$; $\cos\theta$ changes sign upon the transition from $\theta < 90°$ to $\theta > 90°$. In addition, the treatment of bending energy in sections 2 and 3 presumes that R_{12} changes sign when the inner phase is replaced by the outer phase, i.e., for a transition from the emulsion 1-in-2 to emulsion 2-in-1. The latter relations were taken into account when determining the sign of ΔW_b in Table 1. (To avoid misunderstandings, note that R_{12} and ϵ have been presumed to be always positive in the derivation of the expression for W_1, W_2, and Δw in sections 4 and 5.)

For $\varphi_1 \leq \varphi_2$ (Figure 12a), we have the *normal* situation illustrated in Figure 1: the monolayers curve such that the larger area of the particle surface remains on the external side. In this case, s*table* emulsions 1-in-2 and 2-in-1 are formed, respectively, for $\theta \leq 90°$ and $\theta > 90°$. The emulsification work, $w(\theta)$, determines the type of the formed emulsion, while the sign of the bending energy, $\Delta W_b(\theta) > 0$, implies that the produced emulsion will not be flocculated. In this case, the emulsion 1-in-2 is "diluted" ($\varphi_1 \leq 0.5$), whereas the emulsion 2-in-1 is "concentrated" ($\varphi_2 \geq 0.5$).

For $\varphi_1 > \varphi_2$ (Figure 12b), the predictions of the thermodynamic model are exactly the opposite of that illustrated in Figure 1: flocculated emulsions 2-in-1 and 1-in-2 are formed, respectively, for $\theta \leq 90°$ and $\theta > 90°$. In other words, hydrophilic particles are stabilizing the reverse emulsion, whereas hydrophobic particles are stabilizing the direct emulsion. This is an *anomalous* situation, but in principle, the respective emulsions could be experimentally observed if their kinetic stability is sufficiently high. For $\varphi_1 > \varphi_2$, the emulsion 1-in-2 is "concentrated" ($\varphi_1 > 0.5$), whereas the emulsion 2-in-1 is "diluted" ($\varphi_2 < 0.5$).

Because both Δw and ΔW_b depend on θ, it would be correct to say that the contact angle θ (rather than Δw or ΔW_b, alone) controls the properties of the formed emulsions.

Irrespective of the value of θ, the transition from $\varphi_1 \leq \varphi_2$ to $\varphi_1 > \varphi_2$ should lead to a phase inversion (exchange of the continuous and disperse phases), which is discussed in the next subsection.

5.3. Thermodynamic vs Kinetic Factors. Let us recall that the above predictions follow from a thermodynamic model, which is based on several assumptions. The most important of them are the conditions A, B, and C, formulated in the beginning of section 5.1. Other assumptions are that the particles are monodisperse spheres, and there is no contact-angle hysteresis. Of course, the real systems and processes could differ from the above idealized situation, which would lead to a difference between the predictions of the thermodynamic model and the experimental facts. The role of kinetic factors, which could create such differences, is discussed below.

(A) Slow Particle Adsorption. The experiment[17] (phase 1, water; phase 2, toluene + hydrophobized silica particles) indicates that the catastrophic phase inversion happens at $\varphi_1 \approx 0.7$, rather than exactly at $\varphi_1 = 0.5$, as predicted by the above thermodynamic model. This difference could be due to kinetic effects. Indeed, it is important whether the characteristic time of particle adsorption, τ_a, is smaller than the average period between two consecutive drop collisions, τ_c. If $\tau_a < \tau_c$, the drop surfaces will be covered by adsorbed particles at the moment of their collision, and thus coalescence of the two drops will be prevented. In contrast, if $\tau_a > \tau_c$, such a protection is missing, and one could expect a relatively high coalescence rate in the respective emulsion.

τ_a is controlled by the rate of particle supply from the bulk. Because the particles are much bigger than molecules, and the emulsification happens under conditions of strong agitation (usually, in turbulent regime[43−46]), the flux of particles to the drop surfaces is governed by the hydrodynamic transport, rather than by the diffusion. Furthermore, the hydrodynamic fluxes are expected to be stronger in the continuous phase, than in the drops. For this reason, the supply of particles will be faster (and τ_a

smaller) when the particles are dispersed in the continuous phase. This dynamic effect will favor the formation of the emulsion, for which the particles are in the continuous phase (this is emulsion 1-in-2). As a result, the catastrophic phase inversion will be shifted from $\varphi_1 = 0.5$ (as predicted by thermodynamics) to a greater φ_1, as observed experimentally.

Another factor that affects τ_a is the presence of barriers to particle adsorption at the oil−water interface. For example, electrically charged latex particles in water are repelled by the oil−water interface. Thus, the particles may not overcome the electrostatic barrier to adsorption, although if the barrier is overcome, the particles would form a contact angle $\theta \approx 130°-140°$, i.e., they are hydrophobic (see refs 26 and 28). Such barriers could also lead to differences between the predictions of the thermodynamic model and the experiment.

With the increase of φ_1 (and decrease of φ_2) the concentration of drops in the emulsion 2-in-1 decreases, the probability for drop collisions diminishes, and, consequently, τ_c increases. Thus, it may happen that the kinetic criterion, $\tau_a < \tau_c$, is satisfied for the emulsion 2-in-1, and then its formation becomes kinetically favorable. This could be the reason for the phase inversion at $\varphi_1 \approx 0.7$ observed in ref 17. (Similar is the situation with the common, surfactant stabilized emulsions.) Note, however, that in the case of high kinetic barriers to particle adsorption it may happen that the condition $\tau_a < \tau_c$ is never satisfied for emulsion 1-in-2 or 2-in-1 (or even for both of them), and in such a case Pickering emulsion of the respective type will not be formed. Then, the phase inversion will be a transition from a stable emulsion to phase separation.

(B) Easy Particle Desorption. During the emulsification, or later, during the transportation of the produced emulsion in shear slow, the adsorbed particles could be exposed to strong hydrodynamic stresses, which may cause their detachment from the oil−water interface. From this viewpoint, the particle attachment to the fluid interface is the most stable at $\theta = 90°$.[29] Indeed, for $\theta < 90°$ the barrier to particle desorption into phase 2 becomes lower than that for $\theta = 90°$. Likewise, for $\theta > 90°$ the barrier to particle desorption into phase 1 becomes lower than that for $\theta = 90°$. Hence, from the viewpoint of possible particle detachment in the two neighboring phases, the configuration with $\theta = 90°$ is the optimal (see ref 29 for details). On the other hand, in view of Figure 1 and Table 1, $\theta = 90°$ is a transitional value, around which inversion of the emulsion (rather than stability) should be expected. Hence, the emulsion stability at $\theta = 90°$ is another point of discrepancy between the predictions based on thermodynamic and kinetic considerations. Experimentally, depending on the specific conditions (prevailing thermodynamic or kinetic factors) each of the two opposite trends, in principle, could be realized.

(C) Metastable States. Let us give an example. We prepared a Pickering emulsion stabilized by polystyrene latex particles, which were initially dispersed in the water phase (phase 2). At $\varphi_1 = \varphi_2 = 0.5$ we obtained the reverse emulsion, 2-in-1, in agreement with the fact that for latex particles $\theta > 90°$; see the upper-right box of Table 1. In accordance with Table 1, if we add oil to the produced emulsion (if we work at $\varphi_1 > \varphi_2$), we should obtain the direct emulsion 1-in-2 (the lower-right box of Table 1). However, nothing like that was observed experimentally. Instead, the addition of oil (the dilution of the water drops) produced a greater kinetic stability of the reverse, 2-in-1, emulsion. It seems that the latter emulsion corresponds to a metastable state, which is kinetically stable and is realized experimentally, despite the fact that the state with the 1-in-2 emulsion has lower surface free energy, and from this viewpoint, it should be the thermodynamic equilibrium state.

To summarize, the considered thermodynamic model agrees with the following two basic experimental facts: First, it predicts that that for $\varphi_1 \leq \varphi_2$ (Figure 12a) *stable* emulsions 1-in-2 and 2-in-1 will be formed, respectively, for $\theta \leq 90°$ and $\theta > 90°$. Second, it predicts a catastrophic phase inversion (Table 1). On the other hand, kinetic factors (discussed above) could lead to differences between the experimental situation and the thermodynamic predictions. An example is that the model predicts catastrophic phase inversion at $\varphi_1 = \varphi_2 = 0.5$, while experimentally such transition has been observed at $\varphi_1 \approx 0.7$.[17]

6. Summary and Conclusions

The flexural properties of a particle adsorption monolayer were investigated. If the particle monolayer is *not* closely packed, then the interfacial bending moment and the spontaneous curvature are equal to zero ($B_0 = 0$, $H_0 = 0$), while the bending elastic modulus, k_s, is not zero (see eq 2.18). In this case, the interfacial bending energy, ΔW_b, is small compared to the energy of surface dilatation, ΔW_{dil}, and it does not affect the emulsion stability.

The situation changes if the particle monolayer is closely packed. Then the bending moment, B_0, is not zero (see eq 3.11), and the energies of bending and dilatation, ΔW_b and ΔW_{dil}, are comparable. For contact angle $\theta < 90°$, the bending energy stabilizes the emulsions (Figure 6a), whereas for $\theta > 90°$ the total interfacial energy exhibits a minimum (Figure 6b), and correspondingly, the bending energy could cause flocculation. Qualitatively, this corresponds to the picture in Figure 1.

Further, we considered theoretically Pickering emulsions obtained from the liquid phases 1 and 2; supposedly the particles had been initially dispersed in phase 2. "Emulsion 1-in-2" is the emulsion which corresponds to the Bancroft rule[63] (emulsifier in the continuous phase). "Emulsion 2-in-1" is the emulsion for which the particles are in the drops.

Thermodynamic expressions for the work of emulsification, w, have been derived for both emulsions 1-in-2 and 2-in-1 (eqs 4.17 and 4.28). It turns out that w is dominated by the work for creation of a new oil−water interface and the work for particle adsorption at the drop surfaces. The curvature effects turn out to be a higher order effect ($\propto \epsilon^2$). For this reason, the calculated dependencies $w(\epsilon)$ for emulsions 1-in-2 and 2-in-1 seem very similar; cf. Figures 9a and 11a. With the increase of particle "phobicity" to phase 2, i.e., with the increase of the contact angle θ, the emulsification work decreases, because it becomes increasingly favorable to bring the particles from the bulk of phase 2 to the interface. In this way, the formation of the emulsion 2-in-1 is favored insofar as for $\theta > 90°$ that emulsion is expected to be produced for $\varphi_1 \leq \varphi_2$ (see the last column of Table 1).

Next, a thermodynamic emulsification criterion for Pickering emulsions was formulated: If the difference between the work for formation of emulsion 1-in-2 and emulsion 2-in-1 is negative, $\Delta w < 0$, then the emulsion 1-in-2 will be formed. Alternatively, if $\Delta w > 0$, then the emulsion 2-in-1 will be formed; see eqs 5.2, 5.4, and Figure 12. This criterion predicts a "catastrophic" phase inversion at equal volume fractions of oil and water in the emulsion ($\varphi_1 = \varphi_2 = 0.5$). The thermodynamic reason for this phase inversion is that the leading term in Δw is proportional to $(\varphi_1 - \varphi_2)$. Consequently, it changes sign at $\varphi_1 = \varphi_2 =$

0.5, thus abruptly altering the type of the energetically favorable emulsion. Experimentally, the catastrophic phase inversion happens at a somewhat greater volume fraction of phase 1, say at $\varphi_1 = 0.7$ (ref 17). This could be attributed to kinetic factors, which favor the formation of the emulsion 1-in-2 for $\varphi_1 > 0.5$ (section 5.3).

The developed thermodynamic model predicts that for $\varphi_1 \leq \varphi_2$ (Figure 12a) the situation corresponds to the most typical experimental observations: *stable* emulsions 1-in-2 and 2-in-1 are formed, respectively, for $\theta \leq 90°$ and $\theta > 90°$ (Figure 1). The emulsification work, $w(\theta)$, determines the type of the formed emulsion, while the sign of the bending energy, $\Delta W_b(\theta)$, implies that the produced emulsion is stable (Table 1). In contrast, for $\varphi_1 > \varphi_2$ (Figure 12b), the situation is exactly the opposite of that illustrated in Figure 1: flocculated (unstable) emulsions 2-in-1 and 1-in-2 should be formed, respectively, for $\theta \leq 90°$ and $\theta > 90°$. This is an anomalous situation, but in principle, the respective emulsions could be experimentally observed if they are kinetically stabile.

As both Δw and ΔW_b depend on θ, it turns out that the contact angle θ (rather than Δw or ΔW_b, separately) controls the properties of the formed emulsions. Possible deviations from the predictions of the developed thermodynamic model, due to the influence of kinetic factors, are discussed in section 5.3.

Acknowledgment. This work was supported by Unilever Research US. The authors are indebted to Professor K. Danov, Dr. S. Tcholakova, and Mr. K. Golemanov for their assistance.

LA047793D